Photoinduced Intramolecular Charge Transfer in 4-(Dimethyl)aminobenzonitrile − A Theoretical Perspective

Dmitrij Rappoport and Filipp Furche*

Contribution from the Institut für Physikalische Chemie, Universität Karlsruhe, Kaiserstrasse 12, 76128 Karlsruhe, Germany

Received August 7, 2003; E-mail: filipp.furche@chemie.uni-karlsruhe.de

Abstract: Recent advances in time-dependent density functional theory (TDDFT) have led to computational methods that can predict properties of photoexcited molecules with satisfactory accuracy at comparably moderate cost. We apply these methods to study the photophysics and photochemistry of 4-(dimethyl)-aminobenzonitrile (DMABN). DMABN is considered the paradigm of photoinduced intramolecular charge transfer (ICT), leading to dual fluorescence in polar solvents. By comparison of calculated emission energies, dipole moments, and vibrational frequencies with recent results from transient spectroscopy measurements, a definitive assignment of the electronic and geometric structure of the two lowest singlet excited states of DMABN is possible for the first time. We investigate the mechanism of the ICT reaction by means of minimum energy path calculations. The results confirm existing state-crossing models of dual fluorescence. Our study suggests that analytical TDDFT derivative methods will be useful to predict and classify emissive properties of other donor−acceptor systems as well.

1. Introduction

The discovery of dual fluorescence dates back to 1959, when Lippert studied the emission spectrum of 4-(dimethyl)aminobenzonitrile (DMABN).[1] He observed that, besides the "normal" emission band (B band) which is always present, there is an additional red-shifted emission (A band) if the spectrum is recorded in polar solvents. This band was called "anomalous" because it constituted an obvious exception from the well-established rule by Kasha[2] stating that the fluorescence spectrum is dominated by a *single* band arising from emission from the first excited singlet state. Lippert tentatively ascribed the A band to an intramolecular charge-transfer (ICT) state, whose formation should be favored in polar solvents as compared to the less polar "locally excited" (LE) state giving rise to the B band. In the following years, a number of other compounds exhibiting dual fluorescence were discovered, and DMABN became the paradigm of anomalous emissive behavior. The fact that the emissive properties of these compounds can be controlled by external parameters such as solvent polarity or temperature is important for applications, for example, as a fluorescence marker[3] or in materials sciences.[4] The interest multiplied when it became clear that photoinduced ICT may play a crucial role in biological light-harvesting processes such as photosynthesis.[5,6]

The desire to uncover the reason for the unique photochemical properties of DMABN has triggered a large number of experimental and theoretical studies, and excellent reviews exist.[5,7,8] Nevertheless, even for DMABN, the mechanism of the ICT reaction is still a matter of controversial debate.[9,10] Past years have witnessed the emergence of different "schools" that disagree in their view of the ICT state. In the twisted ICT (TICT) model, which was first put forward by Grabowski et al. in the 1970s[11] and later refined,[9,12–14] a 90° twisted conformation of the Me_2N group in the ICT state is postulated, as suggested by the valence bond (VB) structure in Figure 1. This implies that the coordinate of the ICT reaction is the Me_2N twist angle. On the other hand, the so-called planar ICT (PICT)

(1) (a) Lippert, E.; Lüder, W.; Boos, H. In *Advances in Molecular Spectroscopy*; Mangini, A., Ed.; Pergamon Press: Oxford, 1962; pp 443−457. (b) Lippert, E.; Lüder, W.; Moll, F.; Nägele, W.; Boos, H.; Prigge, H.; Seibold-Blankenstein, I. *Angew. Chem.* **1961**, *73*, 695.
(2) Kasha, M. *Discuss. Faraday Soc.* **1950**, *9*, 14.
(3) (a) Rettig, W.; Lapouyade, R. In *Topics in Fluorescence Spectroscopy*; Lakowitz, J. R., Ed.; Plenum Press: New York, 1994; Vol. 4. (b) Rettig, W.; Baumann, W. *Photochem. Photophys.* **1992**, *6*, 79. (c) Malval, J.-P.; Lapouyade, R. *Helv. Chim. Acta* **2001**, *84*, 2439. (d) Malval, J.-P.; Gosse, I.; Morand, J.-P.; Lapouyade, R. In *Springer Series on Fluorescence*; Kraayenhof, R., Ed.; Springer: Berlin, 2002; Vol. 2, pp 87−100. (e) Kundu, S.; Maity, S.; Bera, S. C.; Chattopadhyay, N. *J. Mol. Struct.* **1997**, *405*, 231. (f) Al-Hassan, K. A.; Khanfer, M. F. *J. Fluoresc.* **1998**, *8*, 139.
(4) (a) LaClair, J. J. *Angew. Chem., Int. Ed.* **1998**, *37*, 325. (b) LaClair, J. J. *Angew. Chem., Int. Ed.* **1999**, *38*, 3045.
(5) Rettig, W. *Angew. Chem., Int. Ed. Engl.* **1986**, *25*, 971.
(6) (a) Bautista, J. A.; Connors, R. E.; Raju, B. B.; Hiller, R. G.; Sharples, F. P.; Gosztola, D.; Wasielewski, M. R.; Frank, H. A. *J. Phys. Chem. B* **1999**, *103*, 8751. See also: Zigmantas, D.; Hiller, R. G.; Yartsev, A.; Sundström, V.; Polívka, T. *J. Phys. Chem. B* **2003**, *107*, 5339. (b) Bixon, M.; Jortner, J.; Michel-Beyerle, M. E. *Biochim. Biophys. Acta* **1991**, *1056*, 301. (c) Gust, D.; Moore, T. A. *Top. Curr. Chem.* **1991**, *159*, 103. (d) Zamaraev, K. I.; Khairutinov, R. F. *Top. Curr. Chem.* **1992**, *163*, 1.
(7) (a) Rettig, W. *Top. Curr. Chem.* **1994**, *169*, 253. (b) Rettig, W.; Maus, M. In *Conformational Analysis of Molecules in Excited States*; Waluk, J., Ed.; Wiley-VCH: New York, 2000; pp 1−55. (c) Herbich, J.; Brutschy, B. In *Electron Transfer in Chemistry*; Balzani, V., Ed.; Wiley-VCH: Weinheim, 2001; Vol. 4, pp 697−741. (d) Grabowski, Z. R.; Rotkiewicz, K.; Rettig, W. *Chem. Rev.* **2003**, *103*, 3899.
(8) Lippert, E.; Bonačić-Koutecký, V.; Heisel, F.; Miehé, J. A. *Adv. Chem. Phys.* **1987**, *68*, 1.
(9) Rettig, W.; Bliss, B.; Dirnberger, K. *Chem. Phys. Lett.* **1999**, *305*, 8.
(10) Zachariasse, K. A. *Chem. Phys. Lett.* **2000**, *320*, 8.
(11) Rotkiewicz, K.; Grellmann, K. H.; Grabowski, Z. R. *Chem. Phys. Lett.* **1973**, *21*, 212. Erratum: **1973**, *19*, 315.
(12) Grabowski, Z. R.; Rotkiewicz, K.; Siemiarczuk, A.; Cowley, D. J.; Baumann, W. *Nouv. J. Chim.* **1979**, *3*, 443.
(13) Grabowski, Z. R. *Pure Appl. Chem.* **1993**, *65*, 1751.
(14) Grabowski, Z. R.; Dobkowski, J. *Pure Appl. Chem.* **1983**, *55*, 245.
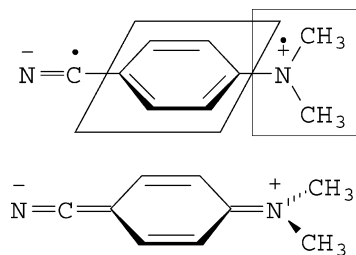
Figure 1. The twisted ICT (upper panel) and planar ICT (lower panel) state models.

model was advocated by Zachariasse and co-workers in a series of papers since 1993.[10,15,16] The basic assumption of the PICT model is a quinoidal ICT state with a planar $Me_2N^+=$ group. As the Me_2N group is slightly pyramidalized in the ground state,[17,18] the ICT reaction coordinate in the PICT model is essentially the Me_2N out-of-plane angle and the quinoidal ring deformation.

The ICT state of DMABN is experimentally well character-ized (see, e.g., refs 5, 8, 19−23). Properties that have been measured so far include vertical absorption and emission energies, dipole moments, polarized fluorescence spectra, and a number of vibrational frequencies. Models are necessary to relate these properties to the electronic and geometric structure of the ICT state. When the qualitative VB picture of Figure 1 is used, the experimental data are hardly sufficient to determine the structure of the ICT state, and they have in fact been interpreted in favor of either model. In recent years, a number of advanced theoretical methods have been applied to the problem. However, for reliable predictions of excited-state structures and other properties, excited-state geometry optimiza-tion is a basic prerequisite, as has also been concluded by Parusel, Rettig, and Sudholt in a recent review of theoretical work on DMABN.[24] So far, applications of correlated ab initio methods to the excited states of DMABN have been seriously hampered by the fact that analytical energy derivative imple-mentations were not available, or the cost was still prohibitive. Geometry optimizations and even (restricted) force constant calculations have been carried out at the configuration interaction

singles (CIS)[25−27] and complete active space self-consistent field (CASSCF) levels of theory.[28] However, these methods do not include (dynamic) correlation effects and are known to have problems with strongly polar excitations. In view of the modest agreement of computed energetics, dipole moments, and force constants with experiments,[27,29] but also with more sophisticated ab initio single-point results,[30−32] these methods are generally not considered accurate enough for definitive conclusions on the nature of the ICT state.

In the present work, we address the problem of photoinduced ICT in DMABN by means of time-dependent density functional methods. While time-dependent density functional theory (TD-DFT) is widely used to calculate vertical excitation spectra, analytical gradient implementations permitting excited-state geometry optimizations and force constant calculations for larger systems have been developed only recently.[33,34] As it has been shown for a set of smaller molecules, TDDFT yields signifi-cantly more accurate excited-state structures, dipole moments, and force constants than CIS, at a quality familiar from ground-state density functional theory (DFT).[33] It is well known that TDDFT tends to underestimate charge-transfer excitation ener-gies considerably[35] due to spurious self-interaction.[36] Single-point TDDFT and DFT/SCI results for DMABN and related systems[20,37−39] indicate, though, that this problem can be controlled when hybrid functionals are used. The focus in the present work is on excited-state properties such as structures and force constants which are generally much less affected by self-interaction than excitation energies.

Apart from its interest for dual fluorescence and DMABN, the present study may be considered as an example of how photochemical problems can be studied by combining theory and experimental results. Reliable theoretical methods are even more important for excited states than for ground states, because experimental data are more difficult to obtain and interpret. Since TDDFT calculations are practicable for systems considerably larger than DMABN, their potential as a tool in theoretical photochemistry deserves some attention.

2. Computational Details

All calculations were performed using Becke's three-parameter hybrid functional (B3-LYP).[40] This choice was motivated by the above-mentioned fact that nonhybrid GGA functionals tend to underestimate excitation energies of charge-transfer states[35] due to spurious

(15) (a) Zachariasse, K. A.; von der Haar, T.; Hebecker, A.; Leinhos, U.; Kühnle, W. *Pure Appl. Chem.* **1993**, *65*, 1745. (b) Zachariasse, K. A.; von der Haar, T.; Leinhos, U.; Kühnle, W. *J. Inf. Record. Mater.* **1994**, *21*, 501. (c) von der Haar, T.; Hebecker, A.; Il'ichev, Y.; Jiang, Y.-B.; Kühnle, W.; Zachariasse, K. A. *Rec. Trav. Chim. Pays-Bas* **1995**, *114*, 430. (d) Zachariasse, K. A.; Grobys, M.; von der Haar, T.; Hebecker, A.; Il'ichev, Y. V.; Kühnle, W.; Morawski, O. *J. Inf. Record. Mater.* **1996**, *22*, 553. (e) Zachariasse, K. A.; Grobys, M.; von der Haar, T.; Hebecker, A.; Il'ichev, Y. V.; Morawski, O.; Rückert, I.; Kühnle, W. *J. Photochem. Photobiol., A* **1997**, *105*, 373.
(16) Zachariasse, K. A.; Grobys, M.; von der Haar, T.; Hebecker, A.; Il'ichev, Y. V.; Jiang, Y.-B.; Morawski, O.; Kühnle, W. *J. Photochem. Photobiol., A* **1996**, *102*, 59.
(17) Heine, A.; Herbst-Irmer, R.; Stalke, D.; Kühnle, W.; Zachariasse, K. A. *Acta Crystallogr., Sect. B* **1994**, *50*, 363.
(18) Kajimoto, O.; Yokoyama, H.; Ooshima, Y.; Endo, Y. *Chem. Phys. Lett.* **1991**, *179*, 455.
(19) Yoshihara, T.; Galievsky, V. A.; Druzhinin, S. I.; Saha, S.; Zachariasse, K. A. *Photochem. Photobiol. Sci.* **2003**, *2*, 342.
(20) Bulliard, C.; Allan, M.; Wirtz, G.; Haselbach, E.; Zachariasse, K. A.; Detzer, N.; Grimme, S. *J. Phys. Chem. A* **1999**, *103*, 7766.
(21) Schuddeboom, W.; Jonker, S. A.; Warman, J. M.; Leinhos, U.; Kühnle, W.; Zachariasse, K. A. *J. Phys. Chem.* **1992**, *96*, 10809.
(22) (a) Herbich, J.; Rotkiewicz, K.; Waluk, J.; Andersen, B.; Thulstrup, E. W. *Chem. Phys.* **1989**, *138*, 105. (b) Fisz, J. J.; van Hoek, A. *Chem. Phys. Lett.* **1997**, *270*, 432. (c) Rettig, W.; Lutze, S. *Chem. Phys. Lett.* **2001**, *341*, 263.
(23) Kwok, W. M.; Ma, C.; Phillips, D.; Matousek, P.; Parker, A. W.; Towrie, M. *J. Phys. Chem. A* **2000**, *104*, 4188.
(24) Parusel, A. B. J.; Rettig, W.; Sudholt, W. *J. Phys. Chem. A* **2002**, *106*, 804.

(25) Scholes, G. D.; Phillips, D.; Gould, I. R. *Chem. Phys. Lett.* **1997**, *266*, 521.
(26) Lommatzsch, U.; Brutschy, B. *Chem. Phys.* **1998**, *234*, 35.
(27) Okamoto, H.; Inishi, H.; Nakamura, Y.; Kohtani, S.; Nakagaki, R. *J. Phys. Chem. A* **2001**, *105*, 4182.
(28) (a) Dreyer, J.; Kummrow, A. *J. Am. Chem. Soc.* **2000**, *122*, 2577. (b) Kummrow, A.; Dreyer, J.; Chudoba, C.; Stenger, J.; Nibbering, E. T. J.; Elsaesser, T. *J. Chin. Chem. Soc.* **2000**, *47*, 721.
(29) Ma, C.; Kwok, W. M.; Matousek, P.; Parker, A. W.; Phillips, D.; Toner, W. T.; Towrie, M. *J. Phys. Chem. A* **2002**, *106*, 3294.
(30) Sobolewski, A. L.; Sudholt, W.; Domcke, W. *J. Phys. Chem. A* **1998**, *102*, 2716.
(31) Sudholt, W.; Sobolewski, A. L.; Domcke, W. *Chem. Phys.* **1999**, *240*, 9.
(32) Sudholt, W. Dissertation; Universität Düsseldorf, 2001.
(33) Furche, F.; Ahlrichs, R. *J. Chem. Phys.* **2002**, *117*, 7433.
(34) (a) van Caillie, C.; Amos, R. D. *Chem. Phys. Lett.* **2000**, *317*, 159. (b) Hutter, J. *J. Chem. Phys.* **2003**, *118*, 3928.
(35) (a) Casida, M. E.; Gutierrez, F.; Guan, J.; Gadea, F.-X.; Salahub, D. R.; Daudey, J.-P. *J. Chem. Phys.* **2000**, *113*, 7062. (b) Dreuw, A.; Weisman, J. L.; Head-Gordon, M. *J. Chem. Phys.* **2003**, *119*, 2043.
(36) Perdew, J. P.; Zunger, A. *Phys. Rev. B* **1981**, *23*, 5048.
(37) Jamorski, C.; Foresman, J. B.; Thilgen, C.; Lüthi, H.-P. *J. Chem. Phys.* **2002**, *116*, 8761.
(38) Jamorski Jödicke, C.; Lüthi, H. P. *J. Am. Chem. Soc.* **2003**, *125*, 252.
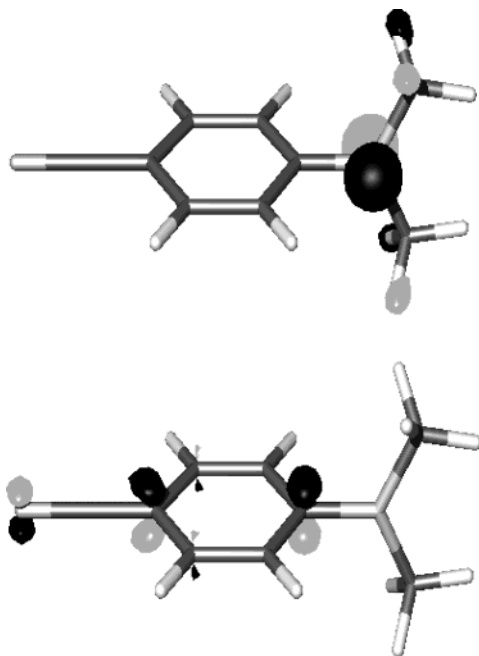(39) Parusel, A. B. J.; Köhler, G.; Grimme, S. *J. Phys. Chem. A* **1998**, *102*, 6297.

Figure 2. HOMO (upper panel) and LUMO (lower panel) at the twisted (ICT) geometry.

self-interaction, which is partly cured by hybridization with Hartree–Fock exchange. Jamorski and Lüthi have pointed out[37,38] that B3LYP yields good agreement with experiment for the vertical excitation energies of the first two excited singlet states; in particular, the energetic separation of the two states is accurately reproduced. Basis sets were of triple-ζ valence quality with two sets of polarization functions (TZVPP)[41] throughout. This extended basis set was chosen for an appropriate treatment of the subtle details of the LE state potential energy surface (see section 4), while most other properties were found to be rather insensitive with respect to the basis set. In exploratory calculations, it was also confirmed that diffuse functions have little effect on the states treated in this work. Fine quadrature grids of size 4 (3 for ground-state calculations)[42] were employed. Vibrational frequencies were determined by numerical differentiation of analytical gradients using central differences and default displacements of 0.02 Bohr.[43] All calculations were carried out using the TURBOMOLE program suite.[44]

3. Results

3.1. The ICT State. According to the TDDFT results, the ICT state of DMABN is the second excited singlet state if the nuclear positions are fixed at the ground-state structure (vertical excitation). Upon optimization, the structure relaxes into a C_{2v}-symmetric minimum with a 90° twisted amino group conformation (Figure 2).

This is accompanied by an increase of the dipole moment and a considerable lengthening of the Ph–N and C≡N bonds by 6.8 and 1.1 pm, respectively. The bond length pattern of the ring is quinoidal. At the excited-state minimum structure, the ICT state is the first excited singlet state and transforms according to the irreducible representation (IRREP) A_2 of C_{2v}.

Table 1. Calculated Properties of the ICT State of DMABN As Compared to Experiment

property[a]	CIS[b]	TDDFT	other	exp.
ΔE (abs.)	5.82	4.67	5.78,[c] 4.39,[d] 4.38,[e] 4.7[f]	4.56[g]
ΔE (emis.)	5.20	2.69		3.05[h]
polarization	long axis	long axis	long axis	long axis
μ	8.9	15.9	15.6[i]	16.1[j]

[a] Energies are in eV, dipole moments are in D. [b] 6-31G** basis, ref 25. [c] CASSCF(12/12), ANO(DZ) basis, ref 32. [d] CASPT2(12/12), ANO(DZ) basis, ref 32. [e] CASPT2(12/9), ANO(DZ) basis, ref 56. [f] STEOM-CCSD, cc-pVTZ basis, ref 57. [g] Electron energy loss (EEL) experiments, ref 20. [h] Fluorescence band maximum in toluene, ref 47. [i] CASSCF(6/5), 6-31G(d) basis, ref 28. [j] Time-resolved microconductivity (TRMC) measurements in 1,4-dioxane, ref 21.

The geometric relaxation is caused by changes in the electronic structure upon excitation of the molecule. The transition may be described as an excitation of an electron from the b_2-symmetric HOMO to the LUMO of b_1 symmetry, as is straightforward from analysis of the computed transition vectors.[45] As shown in Figure 2, the HOMO is essentially a nitrogen p orbital describing the NMe$_2$ lone pair, while the LUMO is a π orbital which is delocalized over the aromatic ring and the C≡N group. It is slightly antibonding with respect to the C≡N triple bond. In the aromatic ring, the LUMO is 1–4-bonding, but weakly antibonding between ring carbon atoms 1 and 2 as well as 1 and 6, which explains the observed bond length pattern. The 1 $^1A_2$ state may thus be considered as a singlet diradical with one unoccupied electron in the HOMO and one in the LUMO. The driving force of the NMe$_2$ twisting is the minimization of the Coulomb interaction between the two unpaired electrons. With increasing twist angle, the HOMO is gradually decoupled from the aromatic π system, which transforms the Ph–N partial double bond into a pure single bond. This mechanism provides a simple rationale for the minimum overlap model,[8,14,46] which has been widely applied to ICT states.

Computed properties of the ICT state are compared to experiment in Table 1. Both absorption and emission energies are in satisfactory agreement with measurements. Computed excitation energies are generally somewhat lower at the twisted structure; this trend is discussed in more detail in section 4. The 1 $^1A_2 \rightarrow$ X transition is electric dipole forbidden; the observed emission band can be explained by "hot" fluorescence from excited vibronic levels, as was first inferred by Grabowski and Rotkiewicz from an analysis of the temperature dependence of the A emission.[13,47] For NMe$_2$ twist angles different from 90°, the transition dipole moment is parallel to the long axis, in accordance with polarized excitation and emission experiments.[22] The exceedingly high dipole moment of ca. 16 D is certainly a characteristic of the ICT state; its absolute value as well as the difference with respect to the ground state is reproduced by the calculations to within experimental accuracy.[48]

(40) Becke, A. D. *J. Chem. Phys.* **1993**, *98*, 5648. In contrast to the Gaussian and Q-Chem implementations, we use the full (beyond RPA) parametrization of the uniform gas correlation energy by Vosko, Wilk, and Nusair (VWN).
(41) Schäfer, A.; Huber, C.; Ahlrichs, R. *J. Chem. Phys.* **1994**, *100*, 5892.
(42) Treutler, O.; Ahlrichs, R. *J. Chem. Phys.* **1995**, *102*, 346.
(43) Considerably smaller displacements are necessary for a reliable prediction of soft modes, especially for the LE state.
(44) Ahlrichs, R.; Bär, M.; Häser, M.; Horn, H.; Kölmel, C. *Chem. Phys. Lett.* **1989**, *162*, 165; see also http://www.turbomole.de.

(45) Furche, F.; Ahlrichs, R.; Wachsmann, C.; Weber, E.; Sobanski, A.; Vögtle, F.; Grimme, S. *J. Am. Chem. Soc.* **2000**, *122*, 1717.
(46) (a) Klessinger, M.; Michl, J. *Excited States and Photochemistry of Organic Molecules*; Wiley: New York, 1995. (b) Bonačić-Koutecký, V.; Koutecký, J.; Michl, J. *Angew. Chem., Int. Ed. Engl.* **1987**, *26*, 170.
(47) Il'ichev, Y. V.; Kühnle, W.; Zachariasse, K. A. *J. Phys. Chem. A* **1998**, *102*, 5670.
(48) The considerable overestimation observed in previous TDDFT studies[37] is mainly due to the use of unrelaxed instead of relaxed densities, which casts some doubt on the validity of this approximation (see also ref 33).

Table 2. Calculated Vibrational Frequencies (cm^{-1}) of the ICT State of DMABN As Compared to Experiment

| | | natural | | ^{15}NMe$_2$ | | (CD$_3$)$_2$ | |
| | | TDDFT | exp.[a] | TDDFT | exp.[a] | TDDFT | exp.[a] |
sym.	assignment						
a$_1$	ν(C≡N)	2218	2095, 2096,[b] 2112[c]	2218	2095	2218	2095
a$_1$	ν(C=C) 8a	1656	1580, 1585[d]	1656	1578	1656	1581
a$_1$	δ(C−H) Me	1501	1502	1500	1504	1143	
a$_1$	ν(C=C) 19a	1470	1358, 1425[e]	1470	1352, 1426[e]	1471	1358, 1426[e]
a$_1$	ν(Ph−N)	1325	1281, 1276[e]	1307	1261, 1262[e]	1281	1249, 1249[e]
b$_2$	δ(C−H) 3, ν(C=C) 14	1305	1276[e]	1305	1280[e]	1306	1274[e]
a$_1$	ν(Ph−CN)	1248	1221, 1220[e]	1247	1221, 1220[e]	1245	1212, 1218[e]
a$_1$	δ(C−H) 9a	1203	1170, 1182[d]	1203	1170	1200	1166
a$_1$	δ(C−H) 20a	1147	1116	1147	1115	1045	1017
a$_1$	δ(C−H) 18a	969	984, 946,[d] 957,[f] 961[g]	969	987	969	985, 957[f]
a$_1$	ν(N−Me)	919	907	912	903	806	801
a$_1$	ring br. 1	766	756	766	755	757	747

[a] Resonance Raman spectrum in methanol from ref 52, unless stated otherwise. [b] Transient IR spectrum in butanol, ref 49. [c] Transient IR spectrum in acetonitrile, ref 50. [d] Resonance Raman spectrum in methanol, ref 23. [e] Transient IR spectrum in acetonitrile, ref 27. [f] Resonance Raman spectrum in methanol, ref 51. [g] Transient IR spectrum in acetonitrile, ref 53.

Table 3. Shift of Vibrational Frequencies (cm^{-1}) of the ICT State Relative to the Ground State

| | natural | | ^{15}NMe$_2$ | | (CD$_3$)$_2$ | |
mode	TDDFT	exp.	TDDFT	exp.	TDDFT	exp.
ν(C≡N)	−103	−124,[a] −102[b,c]	−103	−124[a]	−103	−124[a]
ν(C=C) 8a	−7	−27,[a,d] −22[d,e]	−7	−28[a]	−5	−22[a]
δ(C−H) Me	3	54[a,f]	2	55[a,f]	−27	
ν(C=C) 19a	−94	−169,[a] −104[c,g]	−90	−170,[a] −97[f,g]	−86	−162,[a] −95[f,g]
ν(Ph−N)	−72	−96,[a] −96[c,g]	−73	−103,[a] −94[f,g]	−118	−128,[a] −131[f,g]
δ(C−H) 3, ν(C=C) 14	−41	−52[c,g]	−41	−49[c,g]	−39	−53[c,g]
ν(Ph−CN)	−5	−6,[a,f] −9[c,g]	−6	−6,[a] 4[c,g]	−8	−15,[a] 9[c,g]
δ(C−H) 9a	−8	−10,[a,d] 2[d,e]	−7	−8[a]	−9	−12[a]
δ(C−H) 20a, Me	−53	−63[a]	−53	−56[a,f]	−125	−117[a,f]
δ(C−H) 18a	−60	−19,[a,f] −57,[e,f] −46,[g,h] −44[c,i]	−60	−16[a,f]	−60	−21,[a,f] −49[f,h]
ν(N−Me)	−48	−37[a]	−49	−34[a]	−99	−97[a,c]
ring br. 1	−42	−32[a]	−42	−33[a]	−38	−30[a]

[a] ICT- and ground-state resonance Raman spectra in methanol, ref 52. [b] ICT-state transient IR spectrum in acetonitrile, ref 50. [c] Ground-state IR spectrum in acetonitrile, ref 58. [d] Normal ground-state Raman spectrum in methanol, ref 23. [e] ICT-state resonance Raman spectrum in acetonitrile, ref 23. [f] Normal ground-state Raman spectrum in acetonitrile, ref 58. [g] ICT-state transient IR spectrum in acetonitrile, ref 27. [h] ICT-state resonance Raman spectrum in methanol, ref 51. [i] ICT-state transient IR spectrum in acetonitrile, ref 53.

A specific and detailed characterization of the ICT state is provided by measurements of the excited-state vibrational frequencies. In past years, several groups have reported transient infrared (TIR) and resonance Raman (RR) ICT-state spectra in various polar solvents,[23,27,49-54] including several isotopomers. For assignment purposes, it is advantageous to consider the shifts in vibrational frequencies relative to the ground state, because anharmonicity and solvent effects as well as systematic errors in the computed frequencies tend to cancel by the subtraction. In the following discussion, we will refer to both, absolute ICT-state frequencies in Table 2 and shifts relative to the ground state in Table 3. The agreement of experiment and theory we observe is surprising; the computed shifts in general agree to within ca. 30 cm^{-1} with the measured ones, which is virtually perfect in view of the expected theoretical and experimental inaccuracies. The fact that the calculations accurately reproduce the observed isotopic shifts gives credit to the assignment presented in Table 2. There is a noticeable

exception: the weak feature near 1500 cm^{-1} observed by Kwok and co-workers.[52] The only assignment that can be justified by the calculations, the methyl inversion, leads to an underestimation of the observed shift relative to the ground state by ca. 50 cm^{-1}. We cannot exclude that TDDFT fails here, but the fact that this band has not been observed in all other experimental studies suggests that the problem is not on the theoretical side. A similar comment applies to the band at 1358 cm^{-1} reported by the same authors. In this case, however, TIR results are available[27] that agree much better with the calculations. For the 18a phenyl C−H bending mode, too, the calculations are in favor of TIR[53] and other RR studies.[23,51] The main changes in the vibrational spectrum upon ICT excitation are thus downshifts of the C≡N stretching mode, of the 19a ring stretch, and of the Ph−N stretching mode. This is consistent with a weakening of the corresponding bonds due to the population of the LUMO and also with the calculated changes in the bond lengths.

Geometry optimization of the ICT state using the CIS method leads to a C_1-symmetric minimum with an NMe$_2$ twist angle of ca. 30°.[25,30] As shown in Table 1, the computed vertical emission energy is more than 2 eV too high as compared to experiment, while the dipole moment is ca. 7 D too small. Optimization constrained to C_{2v} symmetry and a 90° NMe$_2$ twist angle results in a saddle point structure[27] with a somewhat higher dipole moment and even higher energy. Not surprisingly, the

(49) Hashimoto, M.; Hamaguchi, H. *J. Phys. Chem.* **1995**, *99*, 7875.
(50) Chudoba, C.; Kummrow, A.; Dreyer, J.; Stenger, J.; Nibbering, E. T. J.; Elsaesser, T.; Zachariasse, K. A. *Chem. Phys. Lett.* **1999**, *309*, 357.
(51) Kwok, W. M.; Ma, C.; Matousek, P.; Parker, A. W.; Phillips, D.; Toner, W. T.; Towrie, M. *Chem. Phys. Lett.* **2000**, *322*, 395.
(52) Kwok, W. M.; Ma, C.; Matousek, P.; Parker, A. W.; Phillips, D.; Toner, W. T.; Towrie, M.; Umapathy, S. *J. Phys. Chem. A* **2001**, *105*, 984.
(53) Okamoto, H. *J. Phys. Chem. A* **2000**, *104*, 4182.
(54) Okamoto, H.; Kinoshita, M.; Kohtani, S.; Nakagaki, R.; Zachariasse, K. A. *Bull. Chem. Soc. Jpn.* **2002**, *75*, 957.

calculated vibrational frequencies show large deviations from experiment and incorrect isotope shifts. For the 90° twisted structure, CIS predicts a Ph−N bond length of only 134 pm, which is almost 10 pm less than the CASSCF and TDDFT values.[55] Geometry optimization at the CASSCF level using a (6/5) reference space leads to a minimum with an NMe_2 twist angle of 90° and a dipole moment of 15.6 D,[28] in agreement with the present TDDFT calculations. The CASSCF structure also shows an elongated Ph−N bond and a quinoidal bond length pattern, although the bond length alternation is less pronounced than that for TDDFT. The CASSCF vibrational frequencies agree well with TDDFT and experiment for the shifts of the $\nu(C\equiv N)$ and $\nu(Ph-N)$ modes relative to the ground state. A detailed comparison with recently available experimental data shows some inconsistencies, however. For example, Okamoto and co-workers have pointed out[27] that the CASSCF vibrational spectrum misses the characteristic 19a ring mode which can be distinguished from methyl bending modes by isotopic substitution. Also, the Ph−CN mode is calculated too low by CASSCF and the shift relative to the ground state has the wrong sign. The two other CASSCF structures reported by Dreyer and Kummrow[28] corresponding to the planar and rehybridized ICT-state models lead to worse agreement of the calculated properties with experiment and are not found to be minima in TDDFT. CASSCF vertical excitation energies for the ICT state are more than 1 eV too high, while more sophisticated methods such as CASSCF plus second-order perturbation theory (CASPT2)[32,56] and similarity transformed equation-of-motion coupled-cluster with single and double excitations (STEOM-CCSD)[57] yield results in good agreement with experiment and TDDFT (Table 1).

In summary, there can be little doubt that the electronic and geometric structure of the ICT state predicted by TDDFT is basically correct. It is noteworthy that the TDDFT result combines certain aspects of the TICT and PICT models that were thought to be contradictory, the twisted amino group conformation and the quinoidal ring structure.

3.2. The LE State. The LE state is the origin of the "normal" B band in the fluorescence spectrum of DMABN; its meta-stability in polar solvents plays a key role for the ICT reaction, as discussed in section 4. A detailed characterization of the LE state is therefore desirable as well. Unfortunately, the amount of experimental data is considerably smaller than that for the ICT state, mainly due to the shorter lifetime of the LE state.

In theory and experiment, the LE state is the lowest excited singlet state of DMABN for vertical excitation at the ground-state structure. In contrast to the ICT state, the energy gain by geometric relaxation is small, as is also reflected by the relatively small difference between absorption and emission energies (Table 4). The main changes in the structure are a considerable elongation of the "quinoidal" bonds between ring atoms 2−3 and 5−6 by 5.5 pm, and a lengthening of the Ph−N bond accompanied by a twisting of the NMe_2 group relative to the

Table 4. Calculated Properties of the LE State of DMABN As Compared to Experiment

property[a]	TDDFT	other	exp.
ΔE (abs.)	4.40	5.88,[b] 4.68,[c] 4.00,[d] 4.19,[e] 4.2[f]	4.25,[g] 4.40, 3.85[h]
ΔE (emis.)	3.76		3.76,[i] 3.63, 3.53[j]
polarization	short axis	short axis	short axis
μ	11.0	9.6[k]	9.7[l]

[a] Units are as in Table 1. [b] CIS, 6-31G** basis, ref 25. [c] CASSCF(12/12), ANO(DZ) basis, ref 32. [d] CASPT2(12/12), ANO(DZ) basis, ref 32. [e] CASPT2(12/9), ANO(DZ) basis, ref 56. [f] STEOM-CCSD, cc-pVTZ basis, ref 57. [g] EEL measurements, ref 20. [h] Absorption band maxima in *n*-hexane and toluene, respectively, refs 47, 59. [i] Maximum of dispersed fluorescence band in supersonic jet, ref 60. [j] Fluorescence band maxima in *n*-hexane and toluene, respectively, refs 47, 59. [k] CASSCF(4/4), 6-31G(d) basis, ref 28. [l] TRMC measurements in cyclohexane, ref 21.
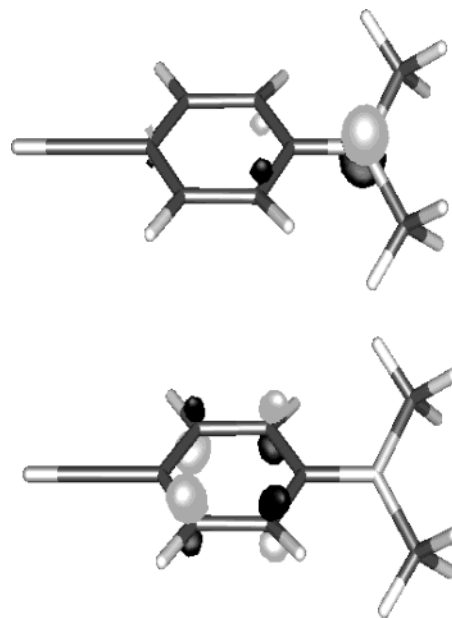

Figure 3. HOMO (upper panel) and LUMO (lower panel) at the geometry of the LE excited state.

ring plane. The energy profile with respect to the NMe_2 twist angle is computed extremely flat for the LE state (see Figure 4); we find shallow minima at 32.5° and 90°, but the energy difference of 0.09 eV is certainly below the accuracy of the method. However, the 90° minimum can be ruled out because its computed dipole moment is 3.5 D too high, while the dipole moment of the minimum at 32.5° agrees reasonably well with the experimental value. An NMe_2 twist angle of ca. 30° is also in accordance with gas-phase absorption measurements[18] by Kajimoto et al.; in contrast, a value of 0° has been inferred from investigations of rotationally resolved laser induced fluorescence.[61]

In terms of Kohn−Sham MOs, generation of the LE state may be described by excitation of an electron from the HOMO to an unoccupied orbital which is the LUMO at the LE state structure and transforms according to the IRREP a of C_2 (Figure 3). This is almost exclusively a π^* orbital of the aromatic

(55) We note that the spin restricted Hartree−Fock ground state is triplet unstable at the twisted geometry, indicating strong static corelation effects in this partial bond breaking situation.
(56) Serrano-Andrés, L.; Merchán, M.; Roos, B. O.; Lindh, R. *J. Am. Chem. Soc.* **1995**, *117*, 3198.
(57) Parusel, A. B. J.; Köhler, G.; Nooijen, M. *J. Phys. Chem. A* **1999**, *103*, 4056.

(58) Okamoto, H.; Inishi, H.; Nakamura, Y.; Kohtani, S.; Nakagaki, R. *Chem. Phys.* **2000**, *260*, 193.
(59) Demeter, A.; Druzhinin, S.; George, M.; Haselbach, E.; Roulin, J.-L.; Zachariasse, K. A. *Chem. Phys. Lett.* **2000**, *323*, 351.
(60) Lommatzsch, U.; Gerlach, A.; Lahmann, C.; Brutschy, B. *J. Phys. Chem. A* **1998**, *102*, 6421.
(61) Pérez Salgado, F.; Herbich, J.; Kunst, A. G. M.; Rettschnick, R. P. H. *J. Phys. Chem. A* **1999**, *103*, 3184.

Table 5. Calculated Vibrational Frequencies (cm^{-1}) of the LE State of DMABN As Compared to Experiment

sym.	assignment	natural		^{15}NMe$_2$		(CD$_3$)$_2$[a]	
		TDDFT	exp.[b]	TDDFT	exp.[d]	TDDFT	exp.[b]
a	ν(C≡N)	2310	2176, 2181[c]	2310		2310	2178
b	δ(C−H) Me	1492	1481[d]	1491	1481	1490 (d2)	
a	ν(C=C) 19a	1523	1467, 1460[c]	1521		1520	1454
a	δ(C−H) Me, δ(C−H) 20a	1447	1416, 1423,[c] 1415[d]	1447	1415	1451 (d2)	1416 (d2)[d]
b	δ(C−H) 3, ν(C=C) 14	1415	1399[d]	1415	1398	1408 (d2)	1398 (d2)[d]
b	δ(C−H) 15	1369	1357	1366		1368	1351
a	ν(Ph−N)	1290	1325, 1334[c]	1278		1247	1285
a	ν(Ph−CN)	1194	1168, 1174[c]	1193		1192	1166
a	ν(C=C) 8a	1160	1113, 1117[c]	1160		1147	1102
a	ν(N−Me)	960	973[c]	953		846	

[a] d2 refers to the 3,5-dideuterated isotopomer. [b] Resonance Raman spectrum in cyclohexane from ref 29, unless stated otherwise. [c] Resonance Raman spectrum in cyclohexane, ref 23. [d] Transient IR spectrum in cyclohexane, ref 54.

Table 6. Shift of Vibrational Frequencies (cm^{-1}) of the LE State Relative to the Ground State

mode	natural		^{15}NMe$_2$		(CD$_3$)$_2$[a]	
	TDDFT	exp.[b]	TDDFT	exp.[b]	TDDFT	exp.[b]
ν(C≡N)	−11	−38,[c] −33[d]	−11		−11	−35[c]
ν(C=C) 19a	−41	−61,[c] −68[d]	−39		−37	−67[c]
δ(C−H) Me, δ(C−H) 20a	−51	−32,[c] −25,[d] −34[e]	−51	−33[e]	−27 (d2)	−17 (d2)[e,f]
δ(C−H) 3, ν(C=C) 14	69	71[e]	69	69[e]	95 (d2)	106 (d2)[e,f]
ν(Ph−N)	−107	−45,[c] −36[d]	−102		−152	−95[c]
ν(Ph−CN)	−59	−59,[c] −53[d]	−60		−61	−63[c]
ν(C=C) 8a	−503	−495,[c] −491[d]	−503		−514	−503[c]
ν(N−Me)	−7	29[d]	−8		−59	

[a] d2 refers to the 3,5-dideuterated isotopomer. [b] Ground-state Raman or IR data in acetonitrile from ref 58 are used, unless stated otherwise. [c] LE state resonance Raman spectrum in cyclohexane from ref 29, unless stated otherwise. [d] LE state resonance Raman spectrum in cyclohexane, ref 23. [e] LE state transient IR spectrum in cyclohexane, ref 54. [f] Ground-state IR spectrum in acetonitrile, ref 54.

system, with a nodal plane between the four central ring carbon atoms. The lengthening of the Ph−N bond and the twisting may thus be attributed to the depopulation of the HOMO, while population of the LUMO leads to the markedly antiquinoidal ring structure. The localization of this orbital in the benzene ring makes a crucial difference to the ICT excitation, where charge is also transferred to the nitrile moiety. Consequently, the dipole moment is lower than that in the ICT state, but still ca. 3 D higher than that in the ground state.

Calculated vibrational frequencies of the LE state are compared to the available experiments in Table 5; again, we also give the shifts relative to the ground state (Table 6). The agreement is in general comparable to that observed for the ICT state, with the exception of the Ph−N stretching mode, which is calculated ca. 70 cm^{-1} too soft. Because two different experiments have led to the same value of ca. 1330 cm^{-1} for this mode, we tend to attribute the discrepancy to the calculation. In fact, the problem may be related to the inability of TDDFT to accurately predict the amino group conformation in the LE state. The most striking feature of the LE state spectrum is an enormous downshift of the "quinoidal" ring stretch 8a by ca. 500 cm^{-1}. In view of the very good agreement of the computed and measured shifts for the natural and the (CD$_3$) isotope substituted species, there can be little doubt that this assignment is correct. The softening of the 8a mode may be understood as an immediate consequence of a population of the LUMO.

In conclusion, the main characteristics of the LE state is its antiquinoidality and the low barrier for the NMe$_2$ rotation. The former seems not to have been generally recognized so far. The picture emerging from both TDDFT calculations and experiment is not compatible with the notion of a "local" excitation in the

NMe$_2$ moiety; the term "locally excited" is therefore justified for historical reasons only.

An LE state geometry optimization at the CIS level has been reported by Ma et al.,[29] imposing C_{2v} symmetry with a planar amino group conformation.[62] The resulting structure is a second-order saddle point, which makes a comparison to experimental data difficult. The computed harmonic frequency shifts are erratic, and the authors conclude that "comparison of experiment with calculated frequencies of much higher accuracy is essential to determine the structure." A planar C_{2v}-symmetric minimum with a dipole moment in reasonable agreement with experiment (Table 4) is found in CASSCF(4/4) calculations.[28] In contrast to the TDDFT structure, the CASSCF structure displays a Ph−N bond shorter than that in the ground state, and a different bond length alternation pattern in the benzene ring roughly corresponding to a localization of negative charge on ring atoms 1, 2, and 6. While the computed CASSCF shift of −29 cm^{-1} in the C≡N stretching frequency compares well with experiment and TDDFT, the shift in the ν(Ph−N) mode of 17 cm^{-1} has the wrong sign; compare Table 6. Moreover, the CASSCF calculations cannot explain the intense band at ca. 1115 cm^{-1} in the RR spectrum of the LE state, which is identified as the quinoidal 8a ring stretch by TDDFT. It therefore appears that important aspects of the LE state, the amino group conformation and the antiquinoidal ring structure, are not adequately reproduced by CASSCF. Higher level ab initio results are available only for vertical excitation energies from

(62) The CIS-optimized "LE state" structures discussed in refs 25 and 26 actually refer to the ICT state, as it follows from the polarization of the computed transition moments.[29,30]

the ground state; both CASPT2[32,56] and STEOM-CCSD[57] give a value of ca. 4.2 eV, close to experiment and TDDFT (Table 4).
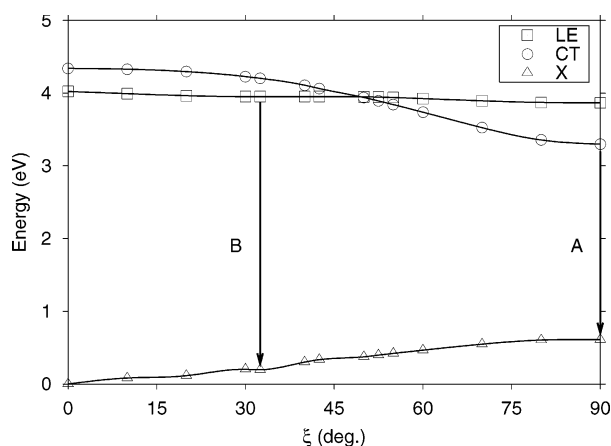

Figure 4. Computed minimum energy profiles for the ICT reaction of DMABN. The structures of the excited states were optimized for each value of ξ; the ground-state energy was evaluated at the geometry of the lowest excited state. The arrows correspond to the B and A emissions observed in the fluorescence spectrum.

4. The ICT Reaction and Dual Fluorescence

In the preceding sections, we have characterized the minima on the two lowest excited potential energy surfaces corresponding to the product and the educt of the ICT reaction LE → ICT. Obviously, the twisted structure of the ICT state suggests the NMe$_2$ twist angle as an appropriate choice for the reaction coordinate ξ. To study the mechanism, we have calculated the minimum energy paths (MEPs) for the ICT and LE states along the reaction coordinate; the results are shown in Figure 4. Each point in Figure 4 corresponds to the result of a geometry optimization where all internal degrees of freedom except ξ are relaxed. The only additional constraint was conservation of C_2 symmetry; this implies that the ICT and LE states can be easily identified for all values of ξ, because they transform according to the two different IRREPs of C_2.

A salient feature of Figure 4 is the intersection of the LE and ICT states at $\xi \simeq 52°$; in this region, strong vibronic coupling can be expected, which allows for transitions between the two states. Another important aspect is the small slope of the LE curve, which is essentially flat. Both observations imply that the LE state minimum is metastable with respect to the ICT-state minimum at $\xi = 90°$. The resulting mechanism can be cast into the following scheme:

$$\text{LE} \underset{k_2}{\overset{k_1}{\rightleftharpoons}} \text{ICT} \qquad (1)$$

$$\text{LE} \overset{k_3}{\longrightarrow} \text{X} \qquad (2)$$

$$\text{ICT} \overset{k_4}{\longrightarrow} \text{X} \qquad (3)$$

Similar mechanisms have been discussed in the literature[5,8,12,13,16,63] for many years. Figure 4 is the result of the first full MEP calculation that provides evidence for this mechanism independent of experiments and ICT-state models. So far, MEP calculations have been carried out at the CIS level only;[30,31]

(63) van der Auweraer, M.; Grabowski, Z. R.; Rettig, W. *J. Phys. Chem.* **1991**, *95*, 2083.

however, CIS fails to predict a state crossing, which again demonstrates the limited accuracy of CIS potential energy surfaces. A number of single-point calculations using unoptimized geometries have been reported, but the corresponding reaction paths generally do not have minimum energy and are therefore somewhat qualitative. Within these limitations, our results confirm previous DFT/SCI[39] and TDDFT[38] single-point results. Single-point CASSCF and CASPT2 calculations based on CIS geometries have been performed by Sobolewski, Sudholt, and Domcke.[30−32] CASSCF does not predict a state crossing, while CASPT2 seems to support the TDDFT picture of Figure 4, in agreement with previous CASPT2[56] and STEOM-CCSD[57] studies. We note that the CASPT2 curves reported in ref 30 deviate to some extent from the TDDFT curves at a larger twist angle, showing an increase in the LE state energy and a rather flat profile for the ICT state. This might indicate a tendency of TDDFT to underestimate the excitation energies at larger ξ. On the other hand, the CIS geometries employed by Sobolewski, Sudholt, and Domcke differ significantly from the TDDFT geometries used in Figure 4 and are likely to differ from CASPT2 geometries, especially at larger ξ (compare section 3.1). For a definite conclusion in this point, correlated ab initio calculations based on geometries of better than CIS quality, for example, from a TDDFT calculation, are necessary. Solvent effects on TDDFT and multireference perturbed CI reaction paths have been studied by Tomasi and co-workers[64,65] using the polarizable continuum model (PCM). While the results are in qualitative agreement with the present study for nonpolar solvents, no state crossing is found in acetonitrile solvent, because the ICT state is calculated lower in energy than the LE state at $\xi = 0$ already. In view of the resulting difficulty to explain the dual fluorescence and the limited accuracy of continuum solvent models, we believe that further work is desirable to confirm this somewhat unexpected result.

A quantitative prediction of the rate constants k_1-k_4 is far beyond our present scope, and we restrict ourselves to some qualitative arguments in the following. The rate constants k_3 and k_4 control the decay of the LE and ICT states to the ground state. k_3 and k_4 are a sum of rate constants for different elementary reactions. Clearly, fluorescence competes with radiationless decay channels. The fluorescence quantum yield for the A emission strongly depends on temperature and solvent polarity,[21,47,66] as expected for an optically forbidden transition.

The energetics of the ICT reaction can be expected to be another important parameter for the emissive behavior of DMABN. Experimental results seem to indicate an equilibrium LE ⇌ ICT in apolar solvents[23] and in the gas phase,[67] while in polar solvents an exponential decay of the LE state in favor of the ICT state is observed.[16,47,68,69] On the other hand, experimental evidence for a barrierless reaction LE → ICT was

(64) Cammi, R.; Menucci, B.; Tomasi, J. *J. Phys. Chem. A* **2000**, *104*, 5631.
(65) Menucci, B.; Toniolo, A.; Tomasi, J. *J. Am. Chem. Soc.* **2000**, *122*, 10621.
(66) (a) Nag, A.; Kundu, T.; Bhattacharyya, K. *Chem. Phys. Lett.* **1989**, *160*, 257. (b) Zachariasse, K. A.; Grobys, M.; Tauer, E. *Chem. Phys. Lett.* **1997**, *274*, 372.
(67) Fuss, W.; Pushpa, K. K.; Rettig, W.; Schmid, W. E.; Trushin, S. A. *Photochem. Photobiol. Sci.* **2002**, *1*, 255.
(68) Leinhos, U.; Kühnle, W.; Zachariasse, K. A. *J. Phys. Chem.* **1991**, *95*, 2013.
(69) Kwok, W. M.; Ma, C.; George, M. W.; Grills, D. C.; Matousek, P.; Parker, A. W.; Phillips, D.; Toner, W. T.; Towrie, M. *Phys. Chem. Chem. Phys.* **2003**, *5*, 1043.

found,[70] with nonexponential kinetics depending on solvent viscosity. Prediction of the ICT reaction energy is difficult due to the mentioned tendency of TDDFT to underestimate excitation energies of CT states; the computed value of −13.9 kcal/mol is therefore expected to be too negative. Nevertheless, we can try to estimate the error by the difference of the errors of the computed vertical emission energies for the ICT and the LE state (in comparison to experimental values for fluorescence maxima in toluene, Tables 1 and 2) to 13.4 kcal/mol. The corrected value of −0.5 kcal/mol is close to zero. Measurements in polar solvents lead to reaction energies of −1.4 to −2.8 kcal/mol (refs 47, 68, see also ref 71). This provides some support for the hypothesis that the ICT reaction is energetically favorable in polar solvents only.[24,71] In view of the inherent inaccuracies of TDDFT and of the neglect of nonadiabatic and solvent effects, a precise estimate of the ICT reaction barrier is beyond our present scope. All we can conclude from the calculations is that the barrier should be small, which agrees with experimental results by Rettig and others (ref 70, see also refs 47, 68).

5. Conclusions and Outlook

We have shown that it is possible to assign the structure of the ICT state of DMABN by combining recent new developments in transient spectroscopy and in time-dependent density functional methods. The same strategy has been applied to obtain a detailed picture of the so-called LE state for the first time. We have been able to extract a mechanism out of the calculations which explains qualitatively the phenomenon of dual fluorescence and is compatible with virtually all experimental kinetic measurements. Whether dual fluorescence can be observed or not depends on the kinetic parameters entering into the mechanism that controls the population of the ICT and LE states and the fluorescence quantum yields. At the present level of TDDFT, it is not possible to predict these parameters without using input from experiments. Nevertheless, it appears plausible that there is a correlation between the energetics of the ICT reaction, which can be estimated from calculations, and the emissive behavior. We suggest that this correlation should be tested for a wider range of dually fluorescent systems in the future, using optimized excited-state structures and including solvent effects. The remarkably successful classification recently proposed by Jamorski and Lüthi[72] is a first step in this direction.

Certainly TDDFT in its present form is not the last word to be said in excited-state theory. More accurate methods such as CC2[73] are needed to calibrate TDDFT results for systems of intermediate size. Another important direction is the improvement of density functionals; for excited states, a practical solution of the self-interaction problem[36] is of primary importance. Nevertheless, as we have demonstrated here, contemporary TDDFT gradient methods are already capable of a degree of accuracy that does provide new insight into excited-state properties and photochemical reactivity, and that represents a substantial improvement over conventional methods such as CIS. In particular, progress in treating excited states of larger molecules can be hoped to result from the combination of transient spectroscopy and TDDFT methods.

We are optimistic that the evidence we have provided for the ICT-state structure is strong enough to put an end to a long and controversial debate. Obviously, a good deal of the TICT-PICT controversy has emerged not from different experimental results, but from disagreement on how to interpret them. Both models, PICT and TICT, were based on oversimplified models of the electronic structure of the ICT state with little or no predictive power. However, there has been some progress in the development of electronic structure theory since Lippert's time. From the present perspective, the question "TICT or PICT?" does not even make sense any more, because it is based on a too simplistic view of reality. The TICT-PICT controversy should be given the place it deserves and become a part of history. The refined theoretical tools that are available now may help us to adopt a new and less biased perspective, and to better understand and exploit the specifics of DMABN and other dually fluorescent molecules.

(70) (a) Heisel, F.; Miehé, J. A. *Chem. Phys.* **1985**, *98*, 233. (b) Heisel, F.; Miehé, J. A.; Marinho, J. M. G. *Chem. Phys.* **1985**, *98*, 243. (c) Rettig, W.; Fritz, R.; Braun, D. *J. Phys. Chem. A* **1997**, *101*, 6830.
(71) Polimeno, A.; Barbon, A.; Nordio, P. L.; Rettig, W. *J. Phys. Chem.* **1994**, *98*, 12158.
(72) (a) Jamorski Jödicke, C.; Lüthi, H. P. *Chem. Phys. Lett.* **2003**, *368*, 561. (b) Jamorski Jödicke, C.; Lüthi, H. P. *J. Chem. Phys.* **2003**, *119*, 12852.
(73) (a) Hättig, C.; Weigend, F. *J. Chem. Phys.* **2000**, *113*, 5154. (b) Köhn, A. Dissertation; Universität Karlsruhe, 2003. (c) Köhn, A.; Hättig, C., in preparation.